

Review

# Radiolabeling of Nucleic Acid Aptamers for Highly Sensitive Disease-Specific Molecular Imaging

Leila Hassanzadeh <sup>1,2</sup> , Suxiang Chen <sup>2,3</sup>  and Rakesh N. Veedu <sup>2,3,\*</sup>

<sup>1</sup> Department of Nuclear Medicine, School of Medicine, Rajaie Cardiovascular, Medical and Research Center & Department of Medicinal Chemistry, School of Pharmacy-International Campus, Iran University of Medical Sciences, Tehran 1449614535, Iran; hassanzadeh.l@iums.ac.ir

<sup>2</sup> Centre for Comparative Genomics, Murdoch University, Perth 6150, Australia; S.Chen@murdoch.edu.au

<sup>3</sup> Perron Institute for Neurological and Translational Science, Perth 6009, Australia

\* Correspondence: R.Veedu@murdoch.edu.au; Tel.: +61-89-360-2803

Received: 22 August 2018; Accepted: 10 October 2018; Published: 15 October 2018



**Abstract:** Aptamers are short single-stranded DNA or RNA oligonucleotide ligand molecules with a unique three-dimensional shape, capable of binding to a defined molecular target with high affinity and specificity. Since their discovery, aptamers have been developed for various applications, including molecular imaging, particularly nuclear imaging that holds the highest potential for the clinical translation of aptamer-based molecular imaging probes. Their easy laboratory production without any batch-to-batch variations, their high stability, their small size with no immunogenicity and toxicity, and their flexibility to incorporate various functionalities without compromising the target binding affinity and specificity make aptamers an attractive class of targeted-imaging agents. Aptamer technology has been utilized in nuclear medicine imaging techniques, such as single photon emission computed tomography (SPECT) and positron emission tomography (PET), as highly sensitive and accurate biomedical imaging modalities towards clinical diagnostic applications. However, for aptamer-targeted PET and SPECT imaging, conjugation of appropriate radionuclides to aptamers is crucial. This review summarizes various strategies to link the radionuclides to chemically modified aptamers to accomplish aptamer-targeted PET and SPECT imaging.

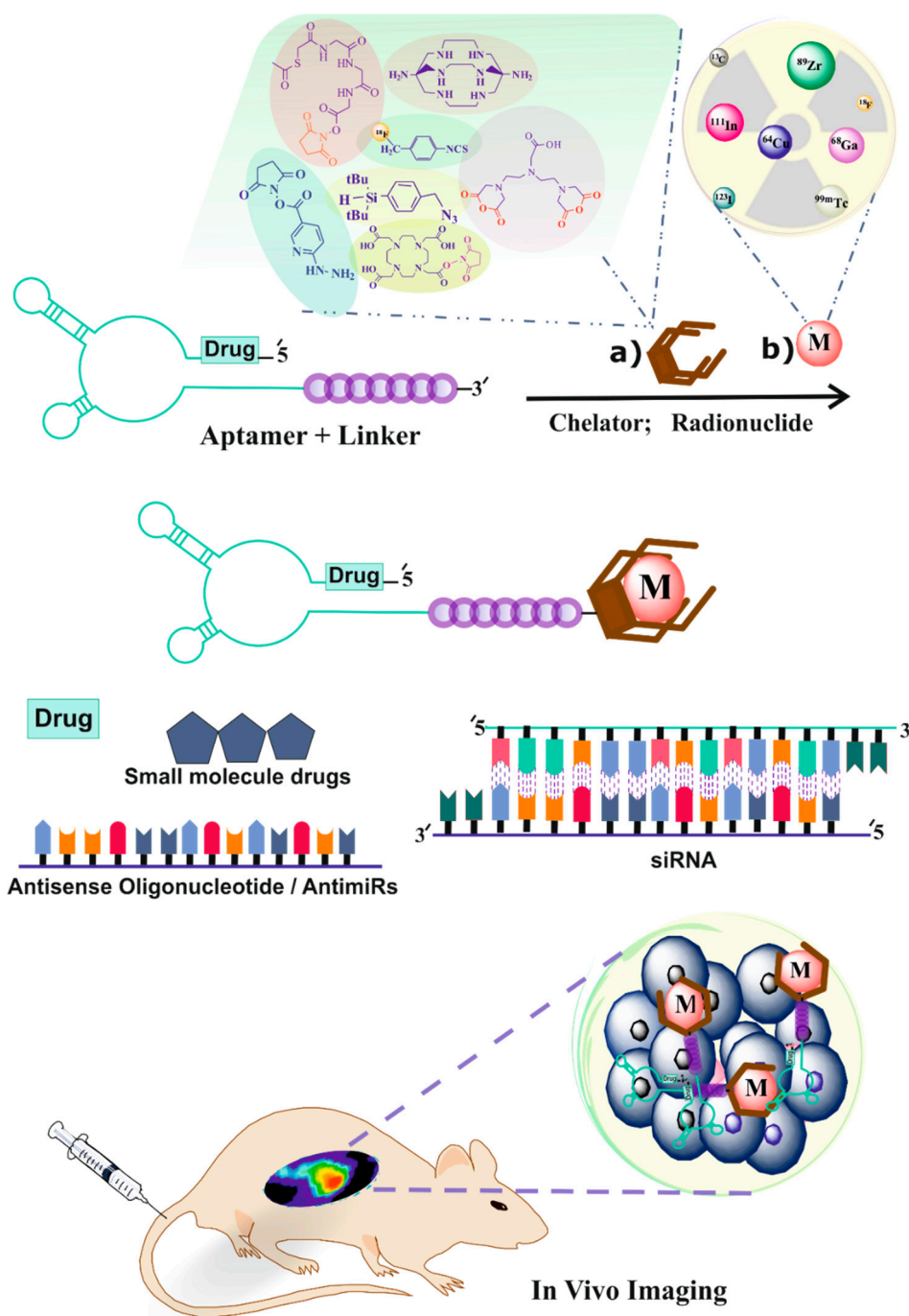
**Keywords:** aptamers; aptamer-targeted imaging; molecular imaging; aptamer-radiolabeling

## 1. Introduction

Molecular imaging technologies employ labeled molecules to explore biological targets in living subjects for disease detection and monitoring treatment progress in real time. The nuclear imaging technique is a powerful approach to achieve highly sensitive imaging. The two most current approaches, that is, positron emission tomography and single photon emission computed tomography, use radionuclides to label specific therapeutic and/or diagnostic (theranostic) molecules for diagnosis and prognosis of many diseases [1,2]. Clinical molecular imaging using these techniques facilitates characterization of biological processes in vivo on a molecular and cellular level [3]. In modern nuclear medicine, approximately 95% of radiopharmaceuticals are used for diagnostic purposes [4]. In addition to small chemical structures, radiopharmaceuticals may consist of bigger biomolecules, such as antibodies, antibody fragments, proteins, peptides, and nucleic acids that are usually more specific [5].

Aptamers are oligomers composed of deoxyribonucleotides (DNA aptamers) or ribonucleotides (RNA aptamers), which are promising targeting biomolecules in nuclear medicine. Various three-dimensional structures of aptamers via intramolecular interactions, such as hydrogen bonds, hydrophobic effects, Vander Waals forces, and so on, enable them to bind the target binding domain

(aptatope) [6]. Aptamers are able to bind different types of targets, such as small ions like  $\text{Zn}^{2+}$ , large targets like proteins, whole cells, bacteria, or viruses [7–10]. These structures can easily differentiate between closely similar molecules, such as the presence or absence of a hydroxyl or methyl group, a urea against a guanidine group, and D or L amino acids that make them highly specific compounds [11–14]. Their high specificity, easy solid phase chemical synthesis, and small size for high tissue penetration make aptamers excellent alternate molecules for use in the medical, pharmaceutical, and biotechnological fields [15]. In this review, we focus on various methods of radiolabeling that have been performed using aptamers and other potential approaches to producing diagnostic tracers in SPECT and PET imaging techniques (Figure 1).



## 2. Improving the Stability of Aptamers

Nucleic acid aptamers composed of natural nucleotide monomers show very low resistance to nucleases and are rapidly degraded *in vivo*. To overcome this significant limitation, chemically-modified nucleotide analogues (Figure 2) are generally systematically incorporated to a developed DNA or RNA aptamer without compromising the target binding affinity and specificity [16]. Some of the prominent modified nucleotides which have been explored in aptamer fabrication are shown in Figure 2. Recently, Lipi et al. provided an in-depth review on developing chemically-modified aptamers [17]. Often termed as ‘chemical antibodies’, aptamers are ideal alternative molecules to antibodies for targeted molecular imaging applications, and several researchers utilized the potential of aptamers in nuclear medicine [18]. Different factors influence the *in-vivo* half-life of the radiolabeled aptamers and alter the biodistribution patterns and clearance pathways, which greatly influence imaging efficiency. Fast clearance of imaging probes might be an advantage because of high target to background ratio. Incorporation of chemically-modified nucleotides certainly improves the properties of aptamers as targeted imaging probes; however, improved nuclease resistance and stability could also enhance the retention time of aptamers and target binding in the body [19].

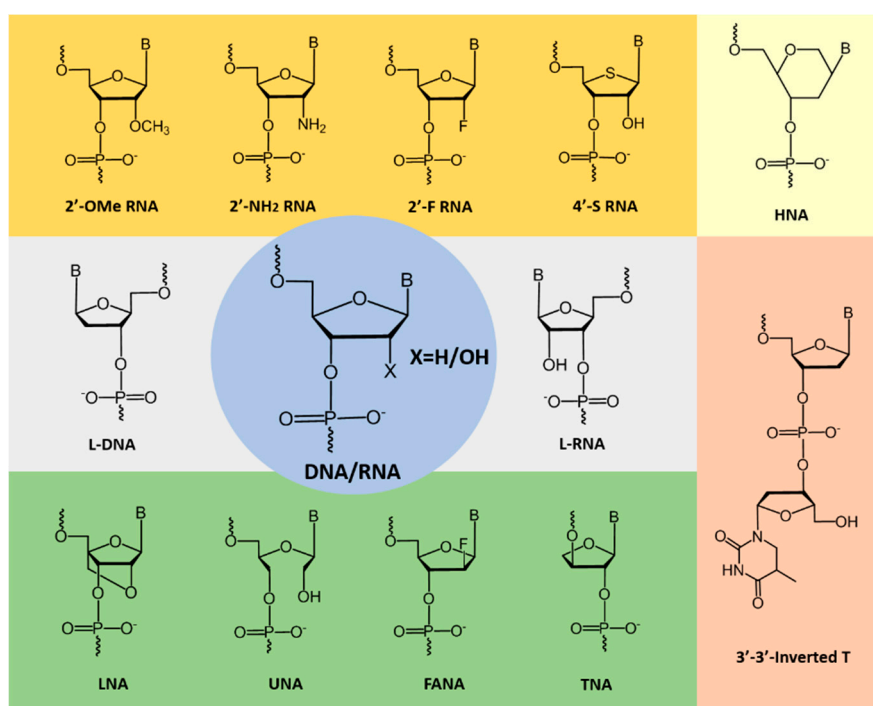


**Figure 2.** Examples of chemically-modified nucleotides used to improve aptamer stability and kinetics.

## 3. SPECT and PET Imaging Techniques

Based on the type of radionuclides used, two types of imaging techniques are employed in nuclear medicine, (1) SPECT (single-photon emission computed tomography), which employs  $\gamma$ -emitting radionuclides, including  $^{99m}\text{Tc}$ ,  $^{123}\text{I}$ ,  $^{67}\text{Ga}$ , and  $^{111}\text{In}$ , and (2) PET (positron emission tomography), which uses  $\beta^+$ -emitting radionuclides, including  $^{18}\text{F}$ ,  $^{11}\text{C}$ ,  $^{13}\text{N}$ ,  $^{15}\text{O}$ ,  $^{68}\text{Ga}$ ,  $^{82}\text{Rb}$ ,  $^{64}\text{Cu}$ , and  $^{89}\text{Zr}$  [4]. Table 1 shows the properties of prominent radionuclides, all of which are diagnostic radionuclides and emit a positron or gamma photon. Each radionuclide has a specific physical half-life, decay mode, chemical properties, and a production method. The physical half-life and decay mode is characteristic for a given radionuclide and non-aligned of any physicochemical condition and cannot be changed with any other method, such as a physicochemical modification. Therefore, it is important to consider the characteristics of radionuclides to target the biological process or disease, which is to be visualized, characterized, or measured [20].

**Table 1.** Characteristics of common nuclear medicine radionuclides [4,20].

Radioisotopes	Atomic Number	Physical Half-Life	Decay Mode (%)
$^{11}\text{C}$	6	20.4 min	$\beta^+$ (100)
$^{13}\text{N}$	7	9.96 min	$\beta^+$ (100)
$^{15}\text{O}$	8	2.03 min	$\beta^+$ (100)
$^{18}\text{F}$	9	109.8 min	$\beta^+$ (97)
$^{62}\text{Cu}$	29	9.76 min	$\beta^+$ (97), EC(3)
$^{64}\text{Cu}$	29	12.8 h	$\beta^+$ Or $\beta^-$ , EC
$^{67}\text{Ga}$	31	3.3 days	EC(100)
$^{68}\text{Ga}$	31	68 min	$\beta^+$ (89), EC(11)
$^{82}\text{Rb}$	37	75 s	$\beta^+$ (95), EC(5)
$^{89}\text{Zr}$	40	78.1 h	$\beta^+$ (23), EC(77)
$^{94\text{m}}\text{Tc}$	43	52 min	$\beta^+$ (72), EC(28)
$^{99\text{m}}\text{Tc}$	43	6.0 h	IT(100)
$^{111}\text{In}$	49	2.8 days	EC(100)
$^{123}\text{I}$	53	13.2 h	EC(100)

$\beta^+$  (Positron), EC (Electron Capture), IT (Isomeric Transition).

## 4. Radio-Labeling of Ligands for SPECT Imaging

### 4.1. $^{99\text{m}}\text{Tc}$ -Radiolabeling

Currently, in most diagnostic nuclear medicine procedures  $^{99\text{m}}\text{Tc}$  is used because of its desirable physical characteristics (half-life: 6.02 h; energy: 140.51 keV and pure gamma emission). Additionally, technetium-99m is readily available in a sterile, pyrogen-free and carrier-free state from  $^{99}\text{Mo}/^{99\text{m}}\text{Tc}$  generators. On the other hand, radio-labeling of aptamers in most situations is a challenging process that needs further chemical synthesis in order to conjugate aptamers to chelating agents, such as Mercaptoacetyltriglycine ( $\text{MAG}_3$ ), Diethylenetriaminepentaacetic acid (DTPA), Hydrazinonicotinamide (HYNIC), and Tetraazacyclododecane tetraacetic acid (DOTA), which have capability to be attached by radioisotopes [21,22]. There are two different methods of  $^{99\text{m}}\text{Tc}$ -labeling for aptamers: (1) Direct method; (2) Indirect method.

#### 4.1.1. Direct $^{99\text{m}}\text{Tc}/^{188}\text{Re}$ Radiolabeling of Aptamers

In this method of radiolabeling,  $^{99\text{m}}\text{Tc}$  without any chelating agent attaches to the biomolecule. It seems to be more favorable because of easy and rapid preparation, less cost and manipulation, and reduction of probable degradation. In 2014, for the first time, the direct  $^{99\text{m}}\text{Tc}$ -labeling of aptamers was reported by Correa C.R. et al. [23]. Two aptamers, with and without primary amine group, were selected and radiolabeled with  $^{99\text{m}}\text{TcO}_4^-$  in the presence of stannous chloride as a reducing agent. The reduction of  $^{99\text{m}}\text{Tc}$  from 7+ oxidation state to a lower oxidation state is required to stimulate a chemical reaction of the  $^{99\text{m}}\text{Tc}$  to many compounds [4]. The aforementioned aptamers were directly labeled with  $^{99\text{m}}\text{Tc}$  by addition of an aliquot of  $\text{Na}^{99\text{m}}\text{TcO}_4$  in the sealed vial, containing Ethylenediamine- $N,N'$ -diacetic acid (EDDA) and tricine. Both aptamers' radiolabeling showed high radiochemical efficiencies and considerable in vitro stability [23]. The next direct radiolabeling of aptamers was performed on several unmodified aptamers with an amine-ended linker by Cao et al. in 2015, and on (1 $\rightarrow$ 3)- $\beta$ -D-glucan aptamers by Sousa Lacerda et al. in 2017 [24,25]. Radiochemical purities that were reported by TLC (thin layer chromatography) indicated high radiolabeling efficiency. Direct radiolabeling of aptamers with Rhenium ( $^{188}\text{Re}$ ) was reported to radiolabel a DNA aptamer to target EGFRvIII for glioblastoma diagnoses by Xidong Wu et al. in 2014. In this method, an aptamer was dissolved in acetic acid (pH 5.0) and radiolabeling was performed in the presence of  $\text{SnCl}_2$  and ascorbic acid, followed by the addition of  $^{188}\text{Re}$  eluent and warming at 37 °C for 1.5 h [26].

#### 4.1.2. Indirect $^{99\text{m}}\text{Tc}$ -Labeling of Aptamers

The labeling of oligomers is performed using a similar strategy to that employed for other biologicals, such as antibodies and peptides. Since  $^{99\text{m}}\text{Tc}$  is an isotope of a metal, the chelator molecule

needs to be attached via a linker to avoid steric hindrances [27]. The  $^{99m}\text{Tc}$  species in a lower oxidation state react chemically with a different type of chelating agents. The chelating agent usually donates lone pairs of electrons to reduced  $^{99m}\text{Tc}$  to generate coordinate covalent bonds [4]. The application of bifunctional chelators such as  $\text{MAG}_3$ , DTPA, and DOTA for radiolabeling oligonucleotides with some radionuclides, are described below [27].

**Mercaptoacetyltriglycine ( $\text{MAG}_3$ ) derivatives:** One of the attractive  $^{99m}\text{Tc}$ -chelators for labeling biomolecules is  $\text{MAG}_3$  that forms stable radioligands in vivo and in vitro without any coligand requirements [28]. Prior to radiolabeling, the tetradentate mercapto-acetyltriglycine is used as its benzyl or benzoyl protected derivative (S-benzoyl or benzyl  $\text{MAG}_3$ ) to avoid the formation of considerable amounts of disulphide-bond, which is removed by heating at 100 °C for 10 min during  $^{99m}\text{Tc}$ -labeling (Figure 3) [29,30]. Rapid deprotection requires higher temperature and alkaline pH [31].

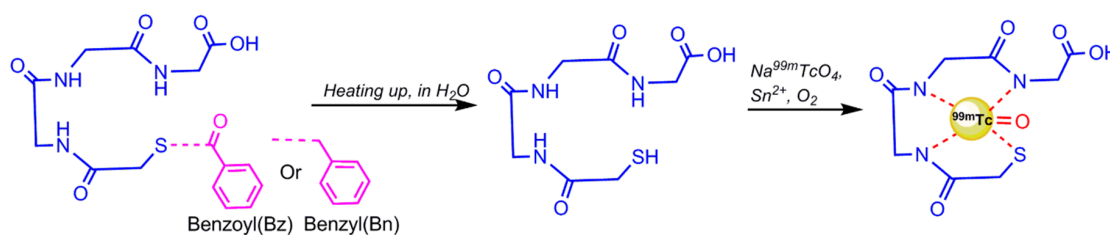


**Figure 3.**  $^{99m}\text{Tc}$  radiolabeling of S-benzoyl Mercaptoacetyltriglycine ( $\text{MAG}_3$ ) chelator.

To avoid the tough conditions of alkaline pH and boiled water temperature of benzoyl deprotection, *N*-hydroxysuccinimidyl S-acetylmercaptoacetyltriglycinate ( $\text{NHS-MAG}_3$ ) was synthesized, in which an acetyl group substituted the benzoyl group. Acetyl as a better leaving group, can be removed at room temperature and neutral pH more easily [32]. The developed  $\text{MAG}_3$  bifunctional chelator (S-acetyl  $\text{NHS-MAG}_3$ ) was used for  $^{99m}\text{Tc}$ -radiolabeling of aptamers and amine derivatized oligonucleotides (Figure 4) [27].

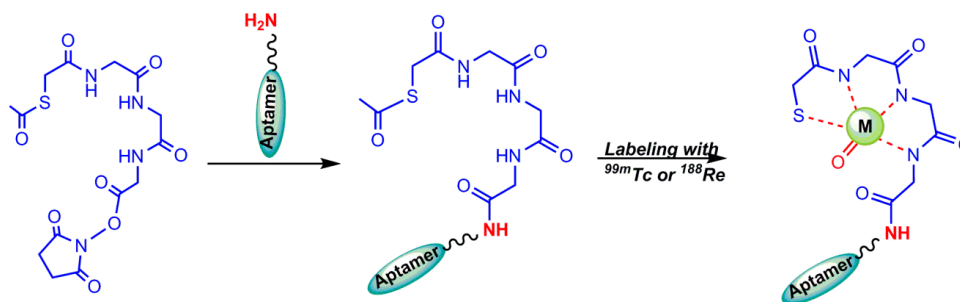


**Figure 4.** Conjugation of the  $\text{NHS-MAG}_3$  chelator to an amine-derivatized aptamer, and radiolabeling.

However, in line with previous reports, postlabeling purification was required to increase the radiochemical purity to 90% or higher, while the labeling of DNAs was performed with  $^{99m}\text{Tc}$  at neutral pH and room temperature [31,33–35]. But, Wang et al. reported the radiolabeling procedure of a 16-mer oligonucleotide with a primary amine group at 5'-end and  $\text{NHS-MAG}_3$  as a bifunctional chelating agent without any purification requirements after labeling [28]. Using  $\text{NHS-MAG}_3$  as bifunctional chelating agents for  $^{99m}\text{Tc}$  radiolabeling of different types of oligonucleotides has been reported in various studies [28,36–39]. The synthesis of  $\text{NHS-MAG}_3$  could be readily conducted according to the procedure described by Winnard et al. [31] or by reacting S-acetylmercaptoacetyltriglycine with *N*-hydroxysuccinimide in the presence of *N,N'*-dicyclohexylcarbodiimide (DCC) as a dehydration reagent in anhydrous *N*-methyl-2-pyrrolidinone (NMP). The conjugation procedure of biomolecule to  $\text{NHS-MAG}_3$  and  $^{99m}\text{Tc}$ -radiolabeling is reported in detail by Wang et al. [28]. A truncated modified RNA aptamer with high affinity for the human matrix metalloprotease 9 (hMMP-9), has been functionalized by conjugating its 5'-end with S-acetylmercaptoacetyltriglycine ( $\text{MAG}_3$ ) through a



hexylamino linker. It was then radiolabeled with  $^{99m}\text{Tc}$  and successfully employed for the detection of hMMP-9 (the tumor biomarker) in human glioblastoma sections (in vitro) and in mice bearing human melanoma tumors (in vivo) [40,41].

**Diethylenetriaminepentaacetic acid (DTPA):** The unshared pair of electrons in the molecules containing  $\text{NH}_3$ ,  $-\text{CN}$ ,  $-\text{SH}$ ,  $-\text{COO}$ ,  $-\text{NH}_2$ , and  $\text{CO}$  can be donated to a metal ion to form a complex. Diethylenetriaminepentaacetic acid (DTPA) and Ethylenediaminetetraacetic acid (EDTA) are usual examples of such chelating agents, with oxygen in carboxyl groups and nitrogen in the amino groups as donor atoms. DTPA has previously been used for radiolabeling antibodies with  $^{99m}\text{Tc}$ , but the resulting radiolabeled ligand was considerably unstable [42]. A covalent coupling method of DTPA to proteins using bicyclic anhydride of DTPA has been reported [43], which was prepared by a one-step synthesis according to the method of Eckelman et al. [44]. The product, when protected from moisture, was stable for many months at room temperature, and the cyclic nature of DTPA anhydride produced by the suggested method above was confirmed by the characteristic evaluation [43]. The cyclic anhydride DTPA has been widely used [43] to radiolabel amine derivatized oligonucleotides with  $^{99m}\text{Tc}$  (Figure 5) [35,45]. Excess amount of anhydride usually is necessary to compensate the hydrolysis of the anhydride that will occur in an aqueous solution in competition with conjugation. DTPA conjugation to DNAs according to the abovementioned method was reported by Hnatowich et al. in 1995 [46].

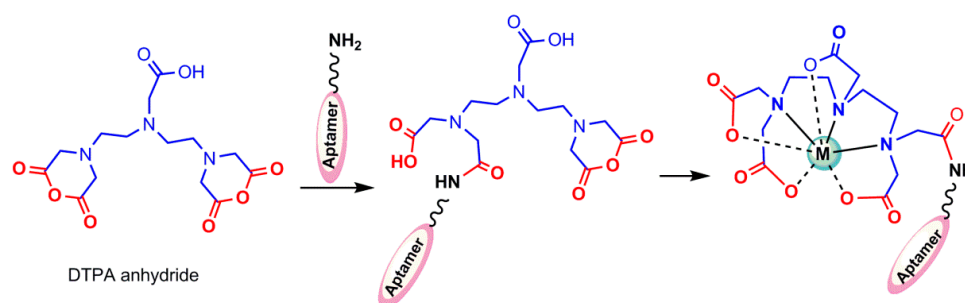


**Figure 5.** Conjugation of the diethylenetriaminepentaacetic acid (DTPA) anhydride to an amine-derivatized aptamer, and radiolabeling.

**Hydrazinonicotinamide (HYNIC):** One of the most useful bifunctional chelating agent used in  $^{99m}\text{Tc}$ -labeling of biomolecules is HYNIC (6-hydrazinopyridine-3-carboxylic acid or hydrazinonicotinamide). The active ester of HYNIC is used to conjugate with the biomolecule—for example, the amino groups of lysine residues in proteins, peptides, or amine-labeled oligonucleotides. HYNIC is able to occupy just two sites of the technetium coordination sphere; coligands such as tricine, EDTA, trisodium triphenylphosphinetrisulfonate (TPPTS) are used to bind other sites and enhance the labeling yield [4]. In 2017, Calzada et al. published a HYNIC-conjugated aptamer radiolabeled with  $^{99m}\text{Tc}$ . A shortened sequence of the original aptamer Sgc8, which has showed similar binding properties to protein kinase 7 membrane receptor, was modified at the 5'-end with an aminohexyl-moiety ( $\text{Sgc8-C}_6\text{-NH}_2$ ) that could be reacted with the bifunctional agent 6-hydrazinonicotinamide succinimidyl ester ( $\text{Suc-HYNIC}$ ) (Figure 6). To synthesize a HYNIC conjugated aptamer, excess amount of  $\text{Suc-HYNIC}$  (in dry DMSO) was added to an aqueous solution of  $\text{Sgc8-C}_6\text{-NH}_2$ . After purification and chemical characterization,  $^{99m}\text{TcO}_4^-$  was used for radiolabeling the HYNIC chelator by incubating with  $\text{SnCl}_2$  and tricine [47]. Another HYNIC conjugation was reported for the AS1411 aptamer targeting nucleolin protein (dissolved in a borate buffer) using  $\text{NHS-HYNIC}$  (in dried dimethylformamide). A purified HYNIC aptamer was dissolved in ammonium acetate and radiolabeled by adding  $^{99m}\text{Tc}$ -pertechnetate solution in the presence of  $\text{SnCl}_2 \cdot 2\text{H}_2\text{O}$  as the reducing agent and tricine as a coligand [48].

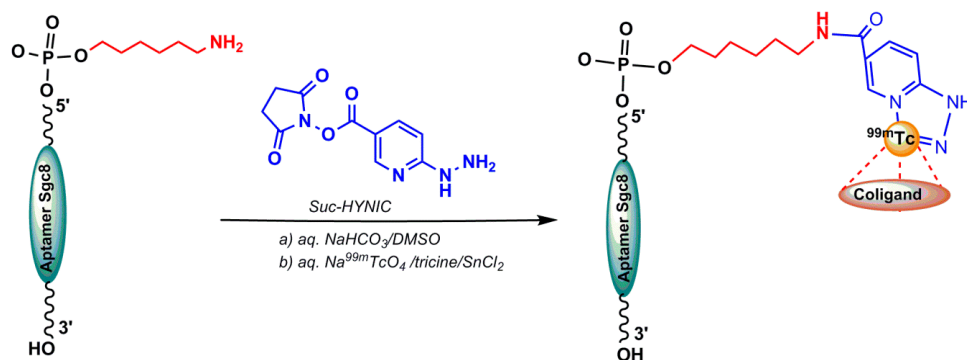


**Figure 6.** Conjugation of the 6-hydrazinonicotinamide succinimidyl ester (Suc–HYNIC) to an amine-derivatized aptamer, and radiolabeling.

*1,4,7,10-Tetraazacyclododecane or 1,4,7,10-tetraacetic acid or Tetraxetan (DOTA):* DOTA, a macrocyclic bifunctional chelating agent, binds to trivalent metals such as Indium ( $\text{In}^{3+}$ ), Yttrium ( $\text{Y}^{3+}$ ), and other metals of lanthanide series rapidly under mild conditions that enable high radiolabeling efficiencies to be achieved at room temperature in comparison with acyclic ligands, such as DTPA. It can be readily modified into a bifunctional chelating agent by the derivatization of one of the carboxylates [49]. Macrocyclic complexes are often extremely resistant to dissociation (macrocyclic effect) because the structures are rather rigid and a great deal of strain in the ligand may need to be overcome in order to break the first metal–donor bond [50]. In 2012, Ren et al. reported the  $^{99\text{m}}\text{Tc}$  radiolabeling of hTERT (human tumor telomerase reverse transcriptase) antisense oligonucleotide (ASON) through the bifunctional chelator DOTA. The ASON sequence, 5'-TAG AGA CGT GGC TCT TGA-3', was conjugated with DOTA–NHS via the amine-functionalization of the oligonucleotides at the 3'-end [51]. DOTA–NHS–ester was prepared using the published procedure [52,53]. In brief, DOTA, 1-(3-Dimethylaminopropyl)-3-ethylcarbodiimide hydrochloride (EDC–HCl) and *N*-hydroxysulfo–succinimide sodium S–NHS were added in PBS (Phosphate Buffered Saline) (pH 5.5). Then, the semistable amino-reactive intermediate DOTA–NHS–ester was added to ASON and radiolabeled by  $^{99\text{m}}\text{TcO}_4^-$  with  $\text{SnCl}_2$  at room temperature (Figure 7). The reported radiochemical purity was 85% [51]. Calzada et al. successfully linked both  $^{99\text{m}}\text{Tc}$  and  $^{67}\text{Ga}$  to an aptamer (Sgc8) through the HYNIC and DOTA chelators, which showed desirable biodistribution and pharmacokinetic properties [47]. In 2018, Dr. Hugo Cerecetto et al. reported the synthetic efforts to prepare conjugates between Sgc8-c (a truncated sequence of the original aptamer Sgc8) and different metallic ion chelator moieties, such as HYNIC, DOTA, and NOTA (1,4,7-triazacyclononane–*N,N',N''*–triacetic acid), were covalently attached at the 5'-end of the aptamer, and were found to be stable in an aqueous solution up to 75 °C for 30 days [54].

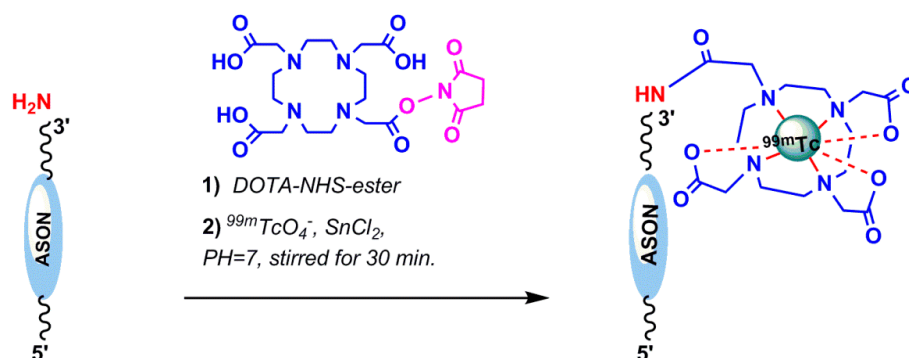


**Figure 7.** Conjugation of the Tetraazacyclododecane tetraacetic acid (DOTA)–NHS–ester to amine-functionalized oligonucleotide for  $^{99\text{m}}\text{Tc}$  radiolabeling.

## 5. Radiolabeling of Ligands for PET Imaging

PET imaging is a sensitive, noninvasive nuclear medicine imaging technique. This technique is able to measure biomedical, pharmacological, and metabolic processes quantitatively in vivo. Consequently, labeling of oligonucleotide with PET radionuclides is a versatile tool to assess the in vivo behavior. Commonly used PET radionuclides are  $^{15}\text{O}$ ,  $^{13}\text{N}$ ,  $^{11}\text{C}$ , and  $^{18}\text{F}$ , with 2.07, 9.97, 20.3, and 110 min half-life, respectively, out of which  $^{18}\text{F}$  has a more favorable half-life [55,56]. Other positron emitting radionuclides are  $^{64}\text{Cu}$ ,  $^{89}\text{Zr}$ , and, most importantly,  $^{68}\text{Ga}$ , which is easily available via a Germanium-68/Gallium-68 Generator in nuclear medicine centers.

### 5.1. $^{18}\text{F}$ Radiolabeling

#### 5.1.1. ( $^{18}\text{F}$ )fluoromethyl)phenyl Isothiocyanate

The possibility of incorporating  $^{18}\text{F}$  into oligonucleotide was reported by Hedberg and Längström in 1997. They developed a one-step synthesis of a labeled compound containing the isothiocyanate functionality ( $^{18}\text{F}$ )fluoromethyl)phenyl isothiocyanate) and investigated the reaction of  $^{18}\text{F}$ -labeled oligonucleotide at 5'-position with a hexylamine linker [57]. The mentioned precursors (1–8) in Figure 8 have been prepared by following the procedure described in the literature [55,57–59]. Isothiocyanates containing leaving groups, such as bromide, iodide, and tosyl, were used as substrates in nucleophilic substitution reactions with  $^{18}\text{F}$ fluoride to produce compound 8 (Figure 8) [57].

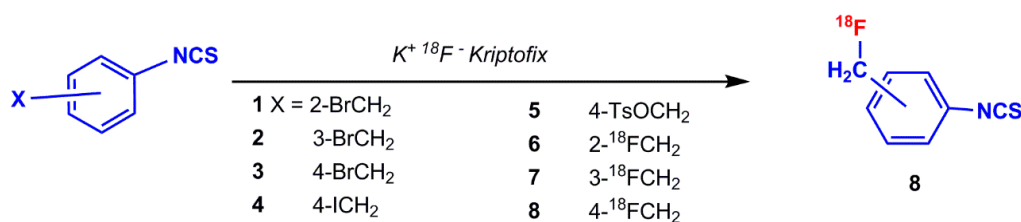


Figure 8. Synthesis of (fluoro- $^{18}\text{F}$ ) ethane isothiocyanatobenzene by various substrates (1–8).

Oligonucleotides can be radiolabeled at 5'-position using ( $^{18}\text{F}$ )fluoromethyl)phenyl isothiocyanate, as shown in Figure 9. In 2003, de Vries et al. reported the  $^{18}\text{F}$ -radiolabeling of ASON using different alkylating agents, and  $N$ -(4- $^{18}\text{F}$ fluorobenzyl)-2-bromoacetamide  $\alpha$ -bromo- $\alpha'$ - $^{18}\text{F}$ fluoro- $m$ -xylene were found to be the most promising [56].

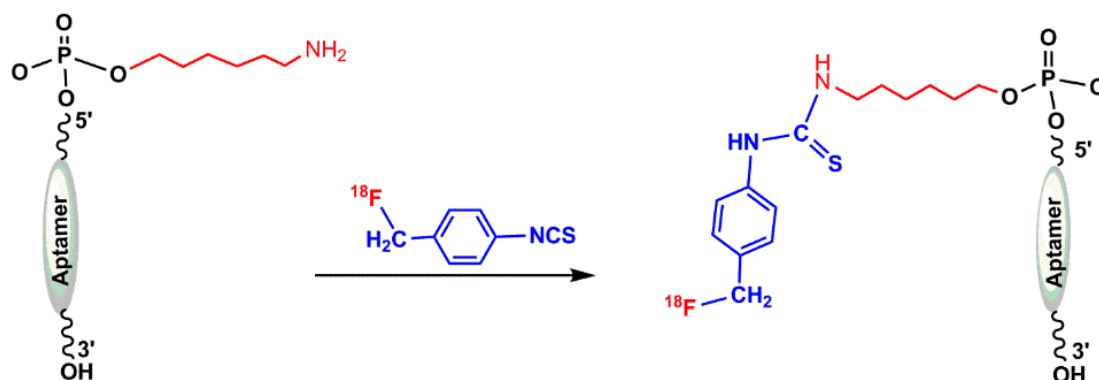


Figure 9. Radiolabeling of 5'-position modified oligonucleotide by ( $^{18}\text{F}$ )fluoromethyl)phenyl isothiocyanate.

#### 5.1.2. Labeling via Click Chemistry Using 1-(Azidomethyl)-4-(Fluoro- $^{18}\text{F}$ ) Benzene

Another reported method for radiolabeling  $^{18}\text{F}$  to aptamers is through the click chemistry approach. Radiolabeling of an Sgc8 aptamer targeting PTK7 was performed using an alkynyl



functionalized Sgc8 aptamer and  $^{18}\text{F}$ -benzylazide via click chemistry. The Sgc8 aptamer was modified at the 5'-end with a terminal hexynyl group and the automated radiochemical synthesis of  $^{18}\text{F}$ -fluorobenzyl azide was achieved using an aromatic fluoride substitution on a spirocyclic hypervalent iodine(III) precursor (Figure 10) [60,61].



**Figure 10.** Conjugation of 1-(azidomethyl)-4-(fluoro- $^{18}\text{F}$ )benzene to a terminal hexynyl modified aptamer.

The abovementioned click reaction protocol was applied for the PET imaging detection of HER<sub>2</sub> in a mouse model with ovarian cancer in 2017 by  $^{18}\text{F}$  radiolabeling of a trivalent HER<sub>2</sub>-targeting aptamer and the alkyne-modified EGFR aptamer (ME07) via click chemistry by Cheng S. et al. in 2018 [62]. The  $^{18}\text{F}$ -benzyl azide precursor has recently indicated robust and reliable radiolabeling with high radiochemical yield [63,64].

#### 5.1.3. Silicon-Based Chemistry for $^{18}\text{F}$ -Radiolabeling

In this method, silylated oligonucleotide was utilized into the  $^{18}\text{F}$ -fluorination reaction (Figure 11). The silylated oligonucleotides were conjugated to different bifunctional silicon building blocks via click chemistry. Under physiological conditions, the di-tertbutylsilyl group is able to be substituted on the silicon atom to stabilize the SiF bond [65,66].

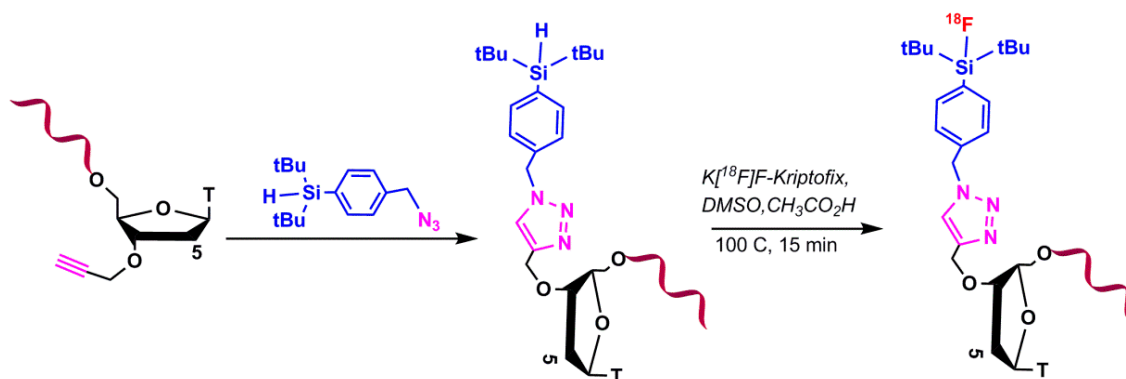


**Figure 11.** Conjugation of  $^{18}\text{F}$  by substitution of hydrogen atom on silylated oligonucleotide.

#### 5.1.4. *N*-Succinimidyl 4- $^{18}\text{F}$ -Fluorobenzoate ( $^{18}\text{F}$ -SFB)

In this method, 2,5-dioxypyrrolidin-1-yl 4-(fluoro- $^{18}\text{F}$ )benzoate ( $^{18}\text{F}$ -SFB) as a precursor of  $^{18}\text{F}$  were used to react with a primary amine functionalized aptamer. In 2015, Jacobson et al. reported  $^{18}\text{F}$ -radiolabeling of a single-stranded DNA aptamer containing 70 nucleotides (Tenascin-C aptamer) using  $^{18}\text{F}$ -SFB. The aptamer was modified to have a 6-carbon chain and only one primary amine group at the 5'-position for conjugation purposes [67]. Radio-synthesis of  $^{18}\text{F}$ -SFB was performed in three automated steps using a 2-reaction-vial module.  $^{18}\text{F}$ -fluoride substitution on *N,N,N*-trimethyl-4-(2,3,4,5,6-pentamethylbenzyl)oxy)carbonyl)benzenaminium (I) was applied in the first reaction vial. The 4-(fluoro- $^{18}\text{F}$ )benzoic acid ( $^{18}\text{F}$ -FBA) was obtained by hydrolysis reaction of 2,3,4,5,6-pentamethylbenzyl 4-(fluoro- $^{18}\text{F}$ )benzoate (II), followed by coupling with bis(2,5-dioxypyrrolidin-1-yl) carbonate and 4-(dimethylamino)pyridine in the second reaction vial to

prepare  $^{18}\text{F}$ -SFB (Figure 12) [68]. The conjugation of  $^{18}\text{F}$ -SFB to an aptamer was performed in a basic sodium phosphate buffer (Figure 13), which resulted in a low but usable yield [67].

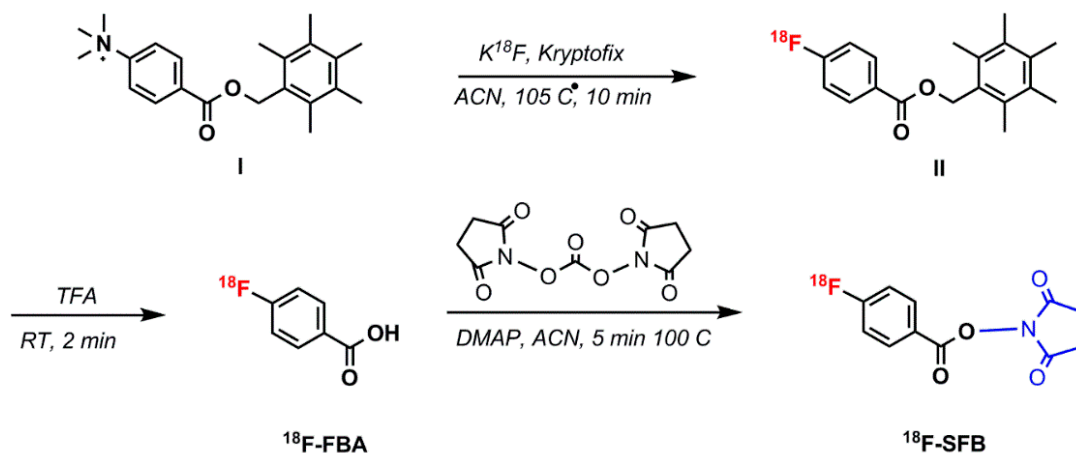


Figure 12. The 3 step synthesis of 2,5-dioxopyrrolidin-1-yl 4-(fluoro- $^{18}\text{F}$ )benzoate ( $^{18}\text{F}$ -SFB).

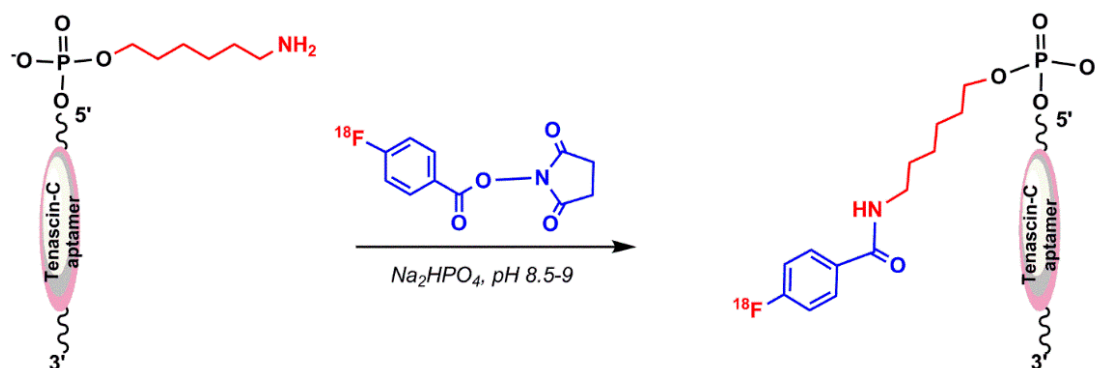


Figure 13. Conjugation of  $^{18}\text{F}$ -SFB to a Tenascin-C aptamer.

#### 5.1.5. Hybridization-Based $^{18}\text{F}$ -Radiolabeling of Aptamers:

Aptamers or aptamer-containing oligonucleotide sequences can be annealed to complementary sequences by following Watson and Crick base-pairing interactions. Park et al. in 2016 reported the development of the complementary oligonucleotide (cODN) hybridization-based aptamer conjugation approach for aptamer-based molecular imaging. The cODN was pre-labeled with  $^{18}\text{F}$  and hybridized with a complementary sequence containing the AS1411 aptamer sequence in an aqueous condition. Briefly, the precursor PEG-mesylate was added to the  $^{18}\text{F}$ -KF- $\text{K}_{222}$  complex and the mixture was stirred at 100 °C for 10 min. Isolated  $^{18}\text{F}$ -PEG-Azide ( $^{18}\text{F}$ -FPA) was reacted with a mixture of 5'-alkyne modified oligonucleotide using *N,N*-diisopropylethylamine and copper (I) iodide in acetonitrile at 70 °C for 20 min. Then, a fully matched sequence (5'-CAG CCA CAC CAC CAG-3') containing the nucleolin aptamer AS1411 sequence was hybridized in an annealing buffer by incubating the mixture at 95 °C for 5 min (Figure 14) [69].

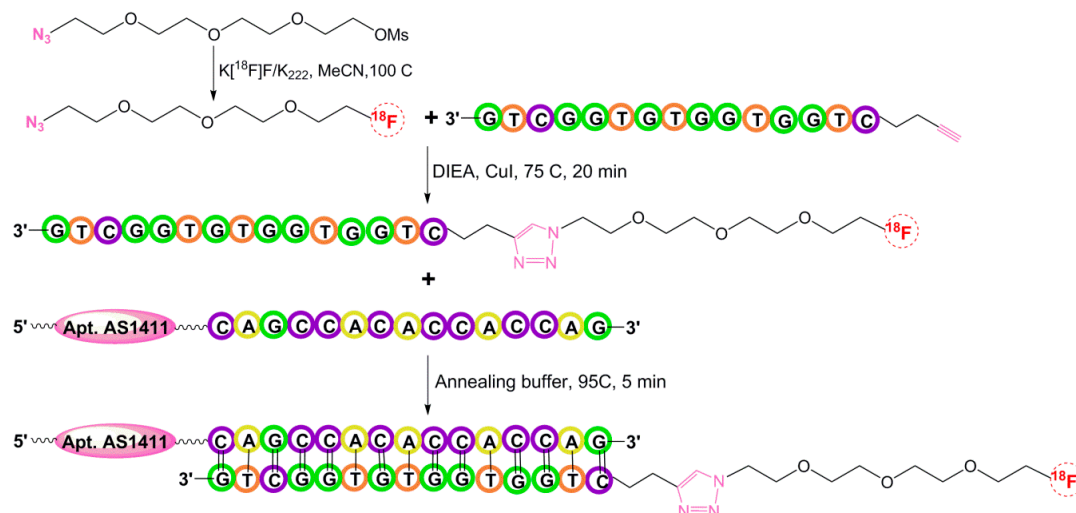


Figure 14. Schematic illustration of Hybridization-based  $^{18}\text{F}$ -Radiolabeling.

### 5.2. $^{64}\text{Cu}$ -Radiolabeling

$^{64}\text{Cu}$  ( $t_{1/2} = 12.7$  h) displays both  $\beta$ -minus decay and positron emission and can be produced with highly specific activity using a medical cyclotron [70–72]. The half-life of this radionuclide enables centralized production and purification for research and clinical studies of targeting molecules, such as peptides and aptamers [73–75]. The optimal labeling with  $^{64}\text{Cu}$  can be achieved under physical conditions in which the oligonucleotides are stable. Based on the chemical properties,  $^{64}\text{Cu}$  is an attractive radionuclide for high-resolution, targeted aptamer-based PET imaging agents [76,77]. In order to radiolabel an aptamer with  $^{64}\text{Cu}$ , it must be linked to a chelator moiety, as shown in Figure 15 [78].

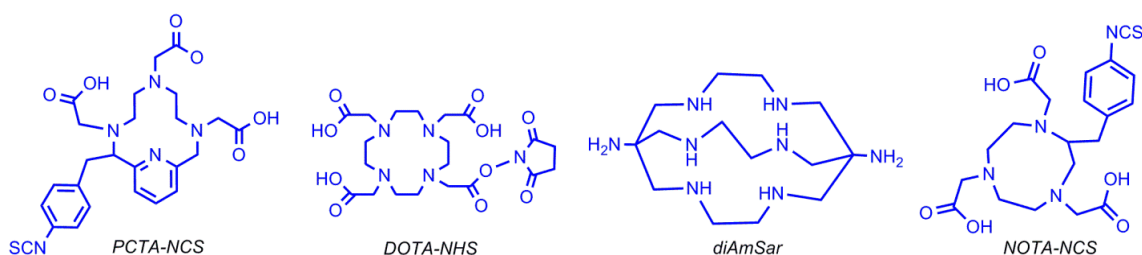


Figure 15. Chelator structures used to conjugate  $^{64}\text{Cu}$  to biomolecules.

Rockey et al. used these different chelators to radiolabel a 5'-amine-modified (12 carbon linker) RNA aptamer that binds PSMA (prostate specific membrane antigen) on prostate cancer cells. Three conjugation strategies were reported: DOTA via the NHS ester, NOTA and PCTA via the 2-S-(4-Isothiocyanatobenzyl) (p-SCN-Bn) linker group, and 1,8-Diamino-3,6,10,13,16,19-hexaazabicyclo[6,6,6]-eicosane(diAmSar) via a disuccinimidyl suberate DSS linker [78]. Paudyal et al. designed and synthesized a radionuclide–chelator–peptide nucleic acid for detecting HER<sub>2</sub> (Human Epidermal Growth Factor Receptor 2) mRNA in malignant breast cancer by PET imaging (Figure 16) [79]. Junling Li et al. reported the labeling of AS1411 (a 26-base guanine-rich oligonucleotide aptamer) with  $^{64}\text{Cu}$  for micro PET/CT study by conjugating four different chelators [80].

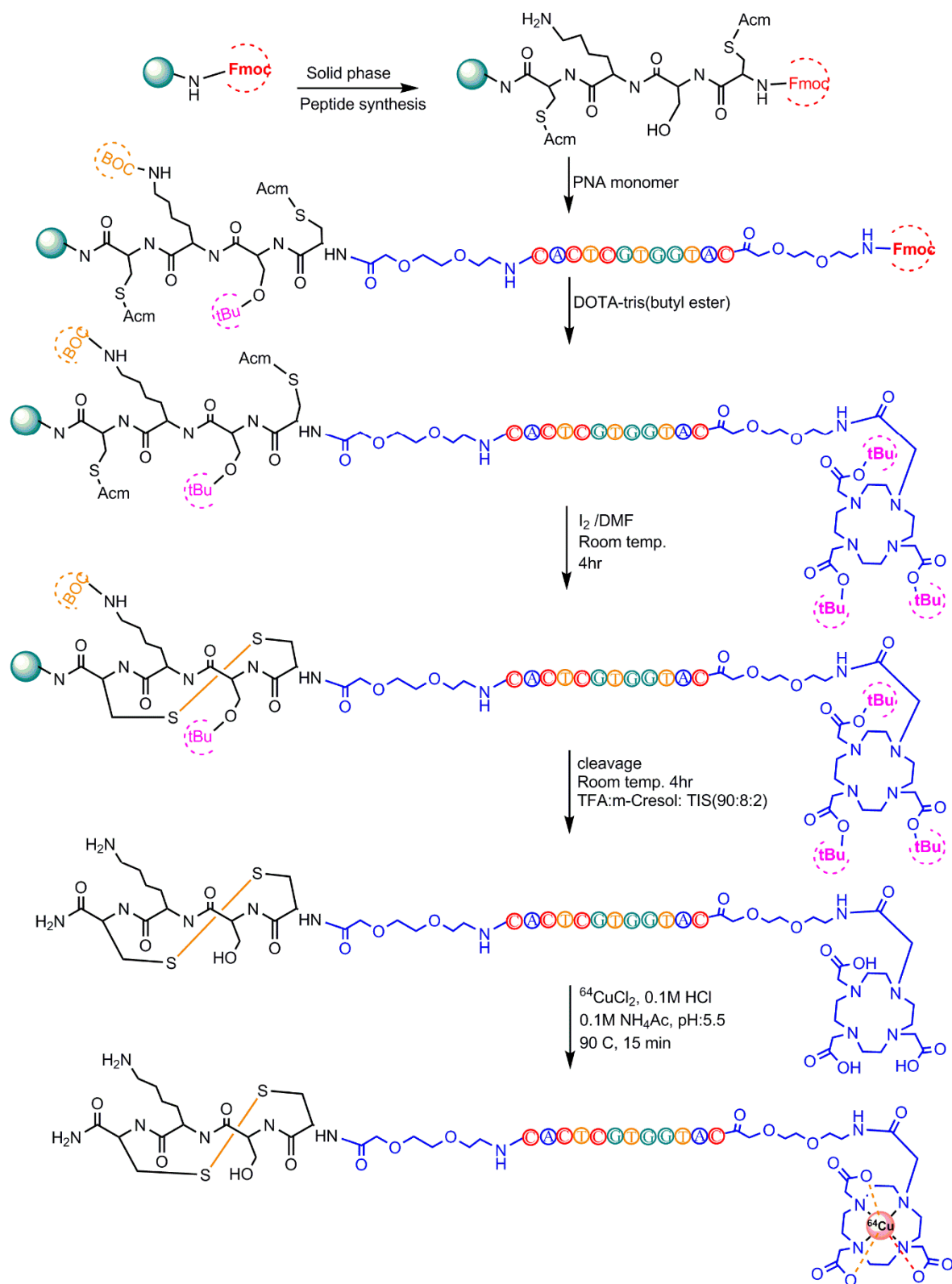
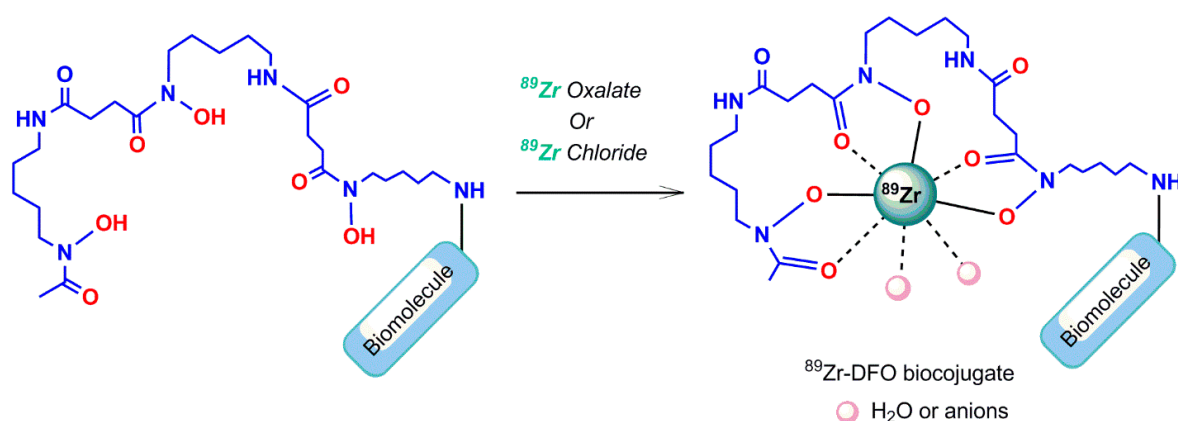


Figure 16.  $^{64}\text{Cu}$ -radiolabeling steps of peptide nucleic acid.

### 5.3. Zirconium-89 Labeling

#### 5.3.1. Desferrioxamine B Chelating Agent

Zirconium-89 ( $^{89}\text{Zr}$ ) has positron emission and favorable half-life of 78.1 h, compared to other  $\beta$ -emitters, which allows long term PET imaging. Because of its adequate half-life and positron emission,  $^{89}\text{Zr}$  is used to radiolabel biomolecules for research human and animal PET imaging, but it has not been yet approved for clinical applications [4]. Although direct labeling methods without using a chelator have been illustrated for  $^{89}\text{Zr}$ -introduction into serum proteins and liposomes, using an appropriate chelator system is a reasonable labeling approach for  $^{89}\text{Zr}$  [81,82].  $^{89}\text{Zr}$  has not shown stable binding to DTPA [83], although it represents a higher stability than the comparable EDTA complex [84].  $^{89}\text{Zr}$  complexation with Desferrioxamine B (a chelating agent exhibiting superior attributes compared to DTPA [83]) is still the frequently used chelator for  $^{89}\text{Zr}$ -radiolabeling and is linked to the biomolecule before performing the radiolabeling reaction. The three hydroxamates and two additional anions or water molecules stabilize the  $\text{Zr}^{4+}$  ion, by the generation of octadentate structural complex in the desferrioxamine B complex (Figure 17) [85].



**Figure 17.** Conjugation of  $^{89}\text{Zr}$  to a Desferrioxamine B (DFO) bioconjugate.

#### 5.3.2. Hyperbranched Polymers (HBPs)

Hyperbranched polymers (HBPs) are the targeted molecular imaging probes, which incorporate both targeting and molecular imaging modalities within one structure [86–88]. Because of their several unique properties, such as tunable solution behavior, critical phase behavior, and presence of large numbers of functional end groups, HBPs are a highly interesting nanocarrier for drug delivery and molecular imaging. The chemical synthesis of different types of branched polymers is reported in the literature [89]. In 2016, Fletcher et al. reported the attachment of an oligonucleotide aptamer with HBPs targeting VEGF (the vascular endothelial growth factors) (VEGF), which are upregulated in triple-negative breast cancer. The attachment of an aptamer to polymer chain was performed by copper-free azide–alkyne 1,3-dipolar cycloaddition. The aptamer–HBP complex was then functionalized with a  $^{89}\text{Zr}$  chelator (desferoxamine) to enable PET imaging with  $^{89}\text{Zr}$  (Figure 18) [90].





labeling of uMUC-1 (underglycosylated mucin-1 (an early marker of tumor development) targeting an aptamer using a p-SCN-bn-NOTA chelating agent [97].

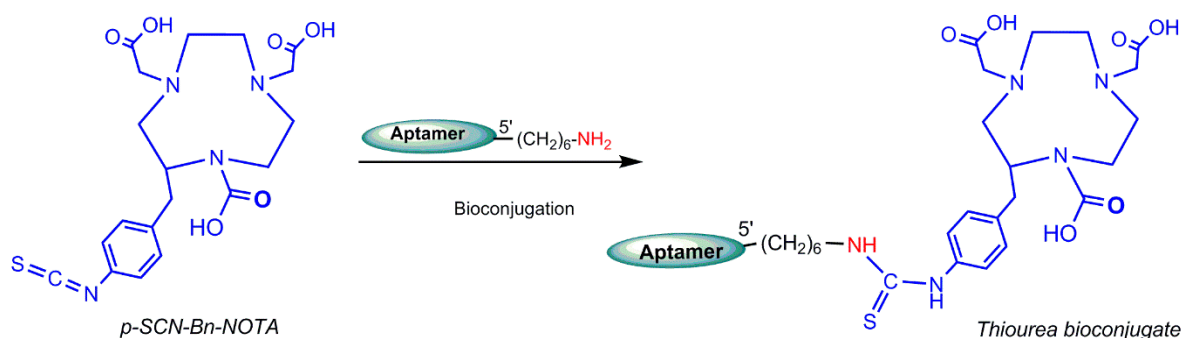


**Figure 19.** Amine–isothiocyanate bioconjugation reaction of isothiocyanate (SCN)–Bn–1,4,7-triazacyclononane– $N,N',N''$ –triacetic acid (NOTA) to a hexylamine-functionalized oligonucleotide.

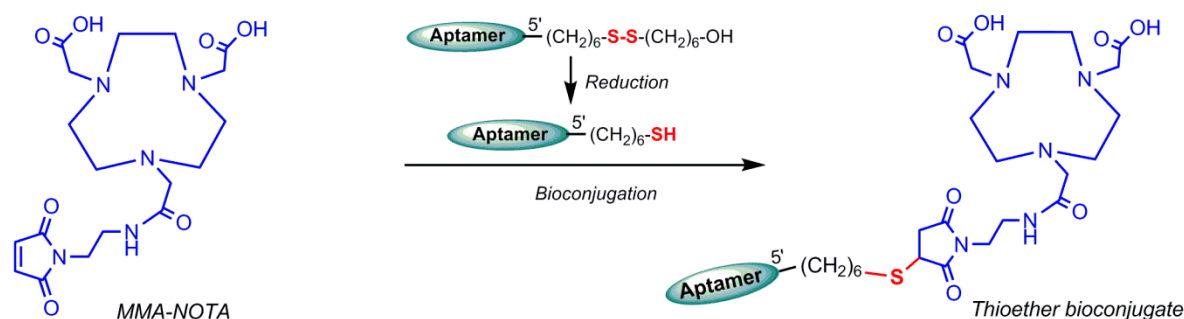


**Figure 20.** Thiol–maleimide bioconjugation reaction of maleimidoethylmonoamide(MMA)–NOTA to a hexylthiol-functionalized oligonucleotide.

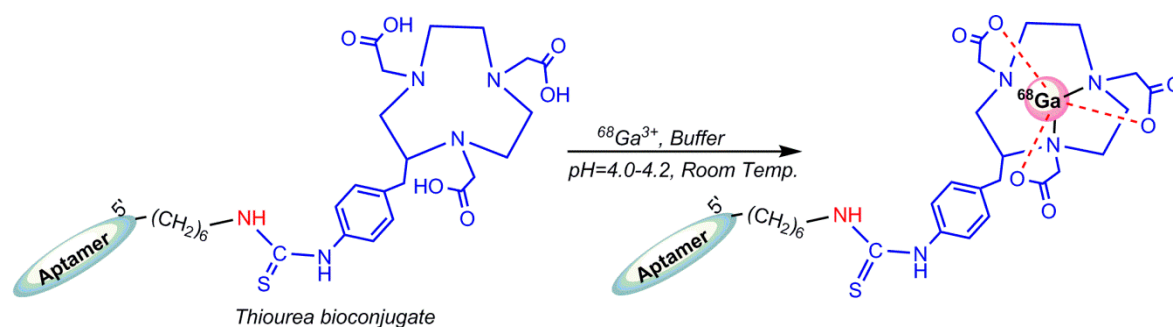


**Figure 21.**  $^{68}\text{Ga}$ -radiolabeling of Thiourea–NOTA–aptamer.

## 6. Conclusions and Future Prospects

Nucleic acid aptamers show high binding affinity to molecular targets with high specificity, which makes them effective biomolecules for generating excellent molecular imaging agents. They require functionalization to generate target-specific molecular imaging probes [98]. One of the most prevalent probe design approaches is the incorporation of functional groups in 5' or 3' ends of aptamers, such as thiols or amines, via phosphoramidite reaction during aptamer synthesis [99]. Despite their many advantages as targeting agents, aptamers possess susceptibility to endogenous nuclease degradation in vivo, and common strategies to overcome this limitation are to enhance nuclease stability by the incorporation of non-natural nucleic acids, such as locked nucleic acids [100–102].

Molecular imaging by aptamers in nuclear tomographic imaging usually requires the covalent attachment of a chelator to the 5' terminal amine of an oligonucleotide aptamer, and then the chelators strongly conjugate radionuclides and feasible nuclear imaging of the molecular target [98].

In this review, the most utilized chelators and radionuclides for generating molecular imaging probes of aptamers as SPECT and PET imaging agents used in recent years have been highlighted. In general, aptamer functionalization may compromise its target affinity. However, in line with the reported literature discussed in this review, it is worth mentioning that radiolabeling of aptamers did not affect the actual aptamer target binding affinity. The literature studies indicated an enhancement of aptamer-targeted SPECT and PET probes and the recent promising results obtained for aptamer-targeted nuclear imaging probes will soon proceed to clinical applications, particularly in the oncology field.

**Author Contributions:** L.H.; writing—original draft preparation, visualization, editing, S.C.; review and editing, R.N.V.; visualization, editing & supervision.

**Funding:** This research was funded by Perron Institute for Neurological and Translational Science.

**Acknowledgments:** R.N.V. greatly acknowledges financial support from McCusker Charitable Foundation and the Perron Institute for Neurological and Translational Science. S.C. thanks the Scholarship support from Murdoch University and Perron Institute for Neurological and Translational Science.

**Conflicts of Interest:** The authors declare no conflict of interest.

## References

1. Luker, G.D.; Piwnica-Worms, D. Molecular imaging in vivo with PET and SPECT. *Acad. Radiol.* **2001**, *8*, 4–14. [[CrossRef](#)]
2. Pimlott, S.L.; Sutherland, A. Molecular tracers for the PET and SPECT imaging of disease. *Chem. Soc. Rev.* **2011**, *40*, 149–162. [[CrossRef](#)] [[PubMed](#)]
3. Thorsten, D.; Viktor, G. Molecular imaging in oncology using positron emission tomography. *Medicine* **2018**, *115*, 175–181.
4. Saha, G.B. *Fundamentals of Nuclear Pharmacy*, 7th ed.; Springer: Basel, Switzerland, 2018; pp. 53–55, 70, 88, 93, 111–112, 148.
5. Aerts, A.; Nren, I.; Gijs, M. Biological carrier molecules of radiopharmaceuticals for molecular cancer imaging and targeted cancer therapy. *Curr. Pharm. Des.* **2014**, *20*, 5218–5244. [[CrossRef](#)] [[PubMed](#)]
6. Gijs, M.; Aerts, A. Aptamers as radiopharmaceuticals for nuclear imaging and therapy. *Nucl. Med. Biol.* **2016**, *43*, 253–271. [[CrossRef](#)] [[PubMed](#)]
7. Bruno, J.G.; Carrillo, M.P. Development, screening, and analysis of DNA aptamer libraries potentially useful for diagnosis and passive immunity of arboviruses. *BMC Res. Notes* **2012**, *5*, 633. [[CrossRef](#)] [[PubMed](#)]
8. Bruno, J.G.; Kiel, J.L. In vitro selection of DNA aptamers to anthrax spores with electrochemiluminescence detection. *Biosens. Bioelectron.* **1999**, *14*, 457–464. [[CrossRef](#)]
9. Ciesiolka, J.; Gorski, J. Selection of an RNA domain that binds  $\text{zn}^{2+}$ . *RNA* **1995**, *1*, 538–550. [[PubMed](#)]
10. Shangguan, D.; Li, Y. Aptamers evolved from live cells as effective molecular probes for cancer study. *Proc. Natl. Acad. Sci. USA* **2006**, *103*, 11838–11843. [[CrossRef](#)] [[PubMed](#)]
11. Famulok, M. Molecular recognition of amino acids by RNA-aptamers: An l-citrulline binding RNA motif and its evolution into an l-arginine binder. *J. Am. Chem. Soc.* **1994**, *116*, 1698–1706. [[CrossRef](#)]
12. Geiger, A.; Burgstaller, P. RNA aptamers that bind l-arginine with sub-micromolar dissociation constants and high enantioselectivity. *Nucleic Acids Res.* **1996**, *24*, 1029–1036. [[CrossRef](#)] [[PubMed](#)]
13. Jenison, R.D.; Gill, S.C. High-resolution molecular discrimination by RNA. *Science* **1994**, *263*, 1425–1429. [[CrossRef](#)] [[PubMed](#)]
14. Sassanfar, M.; Szostak, J.W. An RNA motif that binds ATP. *Nature* **1993**, *364*, 550–553. [[CrossRef](#)] [[PubMed](#)]
15. Famulok, M.; Hartig, J.S. Functional aptamers and aptazymes in biotechnology, diagnostics, and therapy. *Chem. Rev.* **2007**, *107*, 3715–3743. [[CrossRef](#)] [[PubMed](#)]
16. Wang, R.E.; Wu, H.E. Improving the stability of aptamers by chemical modification. *Curr. Med. Chem.* **2011**, *18*, 4126–4138. [[CrossRef](#)] [[PubMed](#)]
17. Lipi, F.; Chen, S. In vitro evolution of chemically-modified nucleic acid aptamers: Pros and cons, and comprehensive selection strategies. *RNA Biol.* **2016**, *13*, 1232–1245. [[CrossRef](#)] [[PubMed](#)]
18. Pang, X.; Cui, C. Bioapplications of cell-selex-generated aptamers in cancer diagnostics, therapeutics, theranostics and biomarker discovery: A comprehensive review. *Cancers* **2018**, *10*, 47. [[CrossRef](#)] [[PubMed](#)]

19. Yoon, S.; Rossi, J. Targeted molecular imaging using aptamers in cancer. *Pharmaceuticals* **2018**, *11*, 71. [[CrossRef](#)] [[PubMed](#)]
20. Lee, Y.S. Radiopharmaceuticals for molecular imaging. *Open Nucl. Med. J.* **2010**, *2*, 178–185. [[CrossRef](#)]
21. Eszter Borbas, K.B.; Catia, S.M.F. Design and synthesis of mono- and multimeric targeted radiopharmaceuticals based on novel cyclen ligands coupled to anti-muc1 aptamers for the diagnostic imaging and targeted radiotherapy of cancer. *Bioconjug. Chem.* **2007**, *18*, 1205–1212. [[CrossRef](#)] [[PubMed](#)]
22. Barros, A.L.B.; Andrade, S.F. Radiolabeling of low molecular weight d-galactose-based glycodendrimer with technetium-99m and biodistribution studies. *J. Radioanal. Nucl. Chem.* **2013**, *298*, 605–609. [[CrossRef](#)]
23. Cristiane, R.C.; Barros, A.L. Aptamers directly radiolabeled with technetium-99m as a potential agent capable of identifying carcinoembryonic antigen (CEA) in tumor cells T84. *Bioorg. Med. Chem. Lett.* **2014**, *24*, 1998–2001.
24. Sousa, L.; Camila, M. (1→3)- $\beta$ -d-glucan aptamers labeled with technetium-99 m: Biodistribution and imaging in experimental models of bacterial and fungal infection. *Nucl. Med. Biol.* **2017**, *46*, 19–24.
25. Santos, S.R.; Rodrigues, C. Identification of staphylococcus aureus infection by aptamers directly radiolabeled with technetium-99m. *Nucl. Med. Biol.* **2015**, *42*, 292–298. [[CrossRef](#)] [[PubMed](#)]
26. Wu, X.; Liang, H. Cell-selex aptamer for highly specific radionuclide molecular imaging of glioblastoma in vivo. *PLoS ONE* **2014**, *9*, e90752. [[CrossRef](#)] [[PubMed](#)]
27. Yuxia, L.; Guozheng, L. A brief review of chelators for radiolabeling oligomers. *Materials* **2010**, *3*, 3204–3217.
28. Wang, Y.; Liu, G. Methods for MAG<sub>3</sub> conjugation and <sup>99m</sup>Tc radiolabeling of biomolecules. *Nat. Protoc.* **2006**, *1*, 1477. [[CrossRef](#)] [[PubMed](#)]
29. Abram, U.; Alberto, R. Technetium and rhenium: Coordination chemistry and nuclear medical applications. *J. Braz. Chem. Soc.* **2006**, *17*, 1486–1500. [[CrossRef](#)]
30. Bormans, G.; Cleynhens, B. Comparison of benzyl, benzoyl and benzamidomethyl as protective groups for mercaptoacetyl triglycine (MAG<sub>3</sub>). *J. Label. Compd. Radiopharm.* **1989**, *26*, 50–52. [[CrossRef](#)]
31. Winnard, P., Jr.; Chang, F. Preparation and use of NHS-MAG<sub>3</sub> for technetium-99m labeling of DNA. *Nucl. Med. Biol.* **1997**, *24*, 425–432. [[CrossRef](#)]
32. Duncan, R.J.; Weston, P.D. A new reagent which may be used to introduce sulfhydryl groups into proteins, and its use in the preparation of conjugates for immunoassay. *Anal. Biochem.* **1983**, *132*, 68–73. [[CrossRef](#)]
33. Liu, G.; Zhang, S. Improving the labeling of s-acetyl NHS–MAG<sub>3</sub>-conjugated morpholino oligomers. *Bioconjug. Chem.* **2002**, *13*, 893–897. [[CrossRef](#)] [[PubMed](#)]
34. Rusckowski, M.; Qu, T. Inflammation and infection imaging with a (<sup>99m</sup>Tc)-neutrophil elastase inhibitor in monkeys. *J. Nucl. Med.* **2000**, *41*, 363–374. [[PubMed](#)]
35. Yu-Min, Z.; Ning, L. Influence of different chelators (HYNIC, MAG3 and DTPA) on tumor cell accumulation and mouse biodistribution of technetium-99m labeled to antisense DNA. *Eur. J. Nucl. Med.* **2000**, *27*, 1700–1707.
36. Kang, L.; Huo, Y. Noninvasive visualization of microRNA-155 in multiple kinds of tumors using a radiolabeled anti-miRNA oligonucleotide. *Nucl. Med. Biol.* **2016**, *43*, 171–178. [[CrossRef](#)] [[PubMed](#)]
37. Kang, L.; Huo, Y. <sup>99m</sup>Tc radiolabeled anti-miR-155 oligonucleotide-phospholipids enveloped nanoparticles for cellular delivery and in vivo imaging. *J. Nucl. Med.* **2017**, *58*, 923.
38. Liu, G.; Dou, S. Radiolabeling of MAG<sub>3</sub>-morpholino oligomers with <sup>188</sup>Re at high labeling efficiency and specific radioactivity for tumor pre-targeting. *Appl. Radiat. Isot.* **2006**, *64*, 971–978. [[CrossRef](#)] [[PubMed](#)]
39. Yan-Rong, Z.; Yong-Xue, Z. Uptake kinetics of <sup>99m</sup>Tc-MAG3-antisense oligonucleotide to PCNA and effect on gene expression in vascular smooth muscle cells. *J. Nucl. Med.* **2005**, *46*, 1052–1058.
40. Gomes, S.D.R. <sup>99m</sup>Tc-MAG<sub>3</sub>-aptamer for imaging human tumors associated with high level of matrix metalloprotease-9. *Bioconjug. Chem.* **2012**, *23*, 2192–2200. [[CrossRef](#)] [[PubMed](#)]
41. Kryza, D.; Debordeaux, F. Ex vivo and in vivo imaging and biodistribution of aptamers targeting the human matrix metalloprotease-9 in melanomas. *PLoS ONE* **2016**, *11*, e0149387. [[CrossRef](#)] [[PubMed](#)]
42. Childs, R.; Hnatowich, D. Optimum conditions for labeling of DTPA-coupled antibodies with technetium-99m. *J. Nucl. Med.* **1985**, *26*, 293–299. [[PubMed](#)]
43. Hnatowich, D.; Layne, W. Radioactive labeling of antibody: A simple and efficient method. *Science* **1983**, *220*, 613–615. [[CrossRef](#)] [[PubMed](#)]
44. Eckelman, W.C.; Karesh, S.M. New compounds: Fatty acid and long chain hydrocarbon derivatives containing a strong chelating agent. *J. Pharm. Sci.* **1975**, *64*, 704–706. [[CrossRef](#)] [[PubMed](#)]

45. Liu, G.; Cheng, D. Replacing  $^{99m}\text{Tc}$  with  $^{111}\text{In}$  improves MORF/cMORF pretargeting by reducing intestinal accumulation. *Mol. Imaging Biol.* **2009**, *11*, 303–307. [[CrossRef](#)] [[PubMed](#)]
46. Hnatowich, D.J.; Winnard, P., Jr. Technetium-99m labeling of DNA oligonucleotides. *J. Nucl. Med.* **1995**, *36*, 2306–2314. [[PubMed](#)]
47. Calzada, V.; Moreno, M. Development of new PTK7-targeting aptamer-fluorescent and-radiolabelled probes for evaluation as molecular imaging agents: Lymphoma and melanoma in vivo proof of concept. *Bioorg. Med. Chem.* **2017**, *25*, 1163–1171. [[CrossRef](#)] [[PubMed](#)]
48. Noaparast, Z.; Hosseinimehr, S. Tumor targeting with a  $^{99m}\text{Tc}$ -labeled as 1411 aptamer in prostate tumor cells. *J. Drug Target.* **2015**, *23*, 497–505. [[CrossRef](#)] [[PubMed](#)]
49. Schlesinger, J.; Fischer, C. Radiosynthesis of new  $^{90}\text{Y}$ -DOTA-based maleimide reagents suitable for the prelabeling of thiol-bearing l-oligonucleotides and peptides. *Bioconjug. Chem.* **2009**, *20*, 1340–1348. [[CrossRef](#)] [[PubMed](#)]
50. Theobald, T. *Sampson's Textbook of Radiopharmacy*; Pharmaceutical Press: London, UK, 2011; p. 96.
51. Ren, B.X.; Yang, F. Magnetic resonance tumor targeting imaging using gadolinium labeled human telomerase reverse transcriptase antisense probes. *Cancer Sci.* **2012**, *103*, 1434–1439. [[CrossRef](#)] [[PubMed](#)]
52. Bartlett, D.W.; Su, H. Impact of tumor-specific targeting on the biodistribution and efficacy of siRNA nanoparticles measured by multimodality in vivo imaging. *Proc. Natl. Acad. Sci. USA* **2007**, *104*, 15549–15554. [[CrossRef](#)] [[PubMed](#)]
53. Lee, H.Y.; Li, Z. PET/MRI dual-modality tumor imaging using arginine-glycine-aspartic (RGD)-conjugated radiolabeled iron oxide nanoparticles. *J. Nucl. Med.* **2008**, *49*, 1371–1379. [[CrossRef](#)] [[PubMed](#)]
54. Sicco, E.; Baez, J. Derivatizations of sgc8-c aptamer to prepare metallic radiopharmaceuticals as imaging diagnostic agents: Syntheses, isolations, and physicochemical characterizations. *Chem. Biol. Drug Des.* **2018**, *91*, 747–755. [[CrossRef](#)] [[PubMed](#)]
55. Nunn, A.D. *Radiopharmaceuticals: Chemistry and Pharmacology*; CRC Press: Boca raton, FL, USA, 1992; Volume 55.
56. de Vries, E.F.; Vroegh, J. Evaluation of fluorine-18-labeled alkylating agents as potential synthons for the labeling of oligonucleotides. *Appl. Radiat. Isot.* **2003**, *58*, 469–476. [[CrossRef](#)]
57. Elisabeth, H.C.; Léngstroma'b, B. Synthesis of 4-([ $^{18}\text{F}$ ] fluoromethyl) phenyl isothiocyanate and its use in labelling oligonucleotides. *Acta Chem. Scand.* **1997**, *51*, 1236–1240.
58. Gonda, J.; Kristian, P. Some nucleophilic reactions of 2-isothiocyanatobenzyl bromide. A new simple synthesis of 2-substituted 4H-benzo [d][1,3] thiazines. *Collect. Czech. Chem. Commun.* **1986**, *51*, 2802–2809. [[CrossRef](#)]
59. Litak, P.T.; Kauffman, J.M. Syntheses of reactive fluorescent stains derived from 5 (2)-aryl-2 (5)-(4-pyridyl) oxazoles and bifunctionally reactive linkers. *J. Hetrocycl. Chem.* **1994**, *31*, 457–479. [[CrossRef](#)]
60. Rotstein, B.H.; Stephenson, N.A.; Vasdev, N.; Liang, S.H. Spirocyclic hypervalent iodine (III)-mediated radiofluorination of non-activated and hindered aromatics. *Nat. Commun.* **2014**, *5*, 4365. [[CrossRef](#)] [[PubMed](#)]
61. Orit Jacobson, I.D.W.; Lu Wang, Z.W.  $^{18}\text{F}$ -labeled single-stranded DNA aptamer for PET imaging of protein tyrosine kinase-7 expression. *J. Nucl. Med.* **2015**, *56*, 1780–1785. [[CrossRef](#)] [[PubMed](#)]
62. Cheng, S.; Jacobson, O.; Zhu, G.; Chen, Z.; Liang, S.H.; Tian, R.; Yang, Z.; Niu, G.; Zhu, X.; Chen, X. PET imaging of EGFR expression using an ( $^{18}\text{F}$ )-labeled RNA aptamer. *Eur. J. Nucl. Med. Mol. Imaging* **2018**. [[CrossRef](#)]
63. Zhu, G.; Zhang, H. Combinatorial screening of DNA aptamers for molecular imaging of HER<sub>2</sub> in cancer. *Bioconjug. Chem.* **2017**, *28*, 1068–1075. [[CrossRef](#)] [[PubMed](#)]
64. James, D.; Escudier, J.M. A 'click chemistry' approach to the efficient synthesis of modified nucleosides and oligonucleotides for PET imaging. *Tetrahedron Lett.* **2010**, *51*, 1230–1232. [[CrossRef](#)]
65. Lucas, R.; Zerrouki, R. A rapid efficient microwave-assisted synthesis of a 3', 5'-pentathymidine by copper (I)-catalyzed [3 + 2] cycloaddition. *Tetrahedron* **2008**, *64*, 5467–5471. [[CrossRef](#)]
66. Sommer, L.; Marans, N. A new reaction in organosilicon chemistry. *J. Am. Chem. Soc.* **1951**, *73*, 882. [[CrossRef](#)]
67. Orit, J.; Xuefeng, Y. PET imaging of tenascin-c with a radiolabeled single-stranded DNA aptamer. *J. Nucl. Med.* **2015**, *56*, 616–621.
68. Jacobson, O.; Weiss, I.D. PET of tumor CXCR<sub>4</sub> expression with 4- $^{18}\text{F}$ -T140. *J. Nucl. Med.* **2010**, *51*, 1796–1804. [[CrossRef](#)] [[PubMed](#)]



69. Park, J.Y.; Lee, T.S. Hybridization-based aptamer labeling using complementary oligonucleotide platform for PET and optical imaging. *Biomaterials* **2016**, *100*, 143–151. [[CrossRef](#)] [[PubMed](#)]
70. Anderson, C.J.; Ferdani, R. Copper-64 radiopharmaceuticals for PET imaging of cancer: Advances in preclinical and clinical research. *Cancer Biother. Radiopharm.* **2009**, *24*, 379–393. [[CrossRef](#)] [[PubMed](#)]
71. Anderson, C.J.; Wadas, T.J. Cross-bridged macrocyclic chelators for stable complexation of copper radionuclides for PET imaging. *Q. J. Nucl. Med. Mol. Imaging* **2008**, *52*, 185–193. [[PubMed](#)]
72. Bass, L.A.; Wang, M. In vivo transchelation of copper-64 from TETA-octreotide to superoxide dismutase in rat liver. *Bioconjug. Chem.* **2000**, *11*, 527–532. [[CrossRef](#)] [[PubMed](#)]
73. Shokeen, M.; Anderson, C.J. Molecular imaging of cancer with copper-64 radiopharmaceuticals and positron emission tomography (PET). *Acc. Chem. Res.* **2009**, *42*, 832–841. [[CrossRef](#)] [[PubMed](#)]
74. Smith, S.V. Molecular imaging with copper-64. *J. Inorg. Biochem.* **2004**, *98*, 1874–1901. [[CrossRef](#)] [[PubMed](#)]
75. Sun, X.; Wuest, M. Radiolabeling and in vivo behavior of copper-64-labeled cross-bridged cyclam ligands. *J. Med. Chem.* **2002**, *45*, 469–477. [[CrossRef](#)] [[PubMed](#)]
76. Cai, H.; Li, Z. Evaluation of copper-64 labeled ambasar conjugated cyclic RGD peptide for improved microPET imaging of integrin  $\alpha v \beta 3$  expression. *Bioconjug. Chem.* **2010**, *21*, 1417–1424. [[CrossRef](#)] [[PubMed](#)]
77. Ferreira, C.L.; Yapp, D.T. Comparison of bifunctional chelates for  $^{64}\text{Cu}$  antibody imaging. *Eur. J. Nucl. Med. Mol. Imaging* **2010**, *37*, 2117–2126. [[CrossRef](#)] [[PubMed](#)]
78. William, M.; Rockey, B. Synthesis and radiolabeling of chelator–RNA aptamer bioconjugates with copper-64 for targeted molecular imaging. *Bioorg. Med. Chem.* **2011**, *19*, 4080–4090.
79. Paudyal, B.; Zhang, K. Determining efficacy of breast cancer therapy by PET imaging of HER2 mRNA. *Nucl. Med. Biol.* **2013**, *40*, 994–999. [[CrossRef](#)] [[PubMed](#)]
80. Li, J.; Zheng, H. Aptamer imaging with cu-64 labeled as 1411: Preliminary assessment in lung cancer. *Nucl. Med. Biol.* **2014**, *41*, 179–185. [[CrossRef](#)] [[PubMed](#)]
81. Abou, D.S.; Thorek, D.L.  $^{89}\text{Zr}$ -labeled paramagnetic octreotide-liposomes for PET-MR imaging of cancer. *Pharm. Res.* **2013**, *30*, 878–888. [[CrossRef](#)] [[PubMed](#)]
82. Meijs, W.E.; Haisma, H.J. A facile method for the labeling of proteins with zirconium isotopes. *Nucl. Med. Biol.* **1996**, *23*, 439–448. [[CrossRef](#)]
83. Meijs, W.E.; Herscheid, J.D. Evaluation of desferal as a bifunctional chelating agent for labeling antibodies with zr-89. *Int. J. Rad. Appl. Instrum. A* **1992**, *43*, 1443–1447. [[CrossRef](#)]
84. Wadas, T.J.; Wong, E.H. Coordinating radiometals of copper, gallium, indium, yttrium, and zirconium for pet and spect imaging of disease. *Chem. Rev.* **2010**, *110*, 2858–2902. [[CrossRef](#)] [[PubMed](#)]
85. Baroncelli, F.; Grossi, G. The complexing power of hydroxamic acids and its effect on the behaviour of organic extractants in the reprocessing of irradiated fuels—I. *J. Inorg. Nucl. Chem.* **1965**, *27*, 1085–1092. [[CrossRef](#)]
86. Fuchs, A.V.; Tse, B.W. Evaluation of polymeric nanomedicines targeted to psma: Effect of ligand on targeting efficiency. *Biomacromolecules* **2015**, *16*, 3235–3247. [[CrossRef](#)] [[PubMed](#)]
87. Pearce, A.K.; Rolfe, B.E. Development of a polymer theranostic for prostate cancer. *Polym. Chem.* **2014**, *5*, 6932–6942. [[CrossRef](#)]
88. Rolfe, B.E.; Blakey, I. Multimodal polymer nanoparticles with combined  $^{19}\text{F}$  magnetic resonance and optical detection for tunable, targeted, multimodal imaging in vivo. *J. Am. Chem. Soc.* **2014**, *136*, 2413–2419. [[CrossRef](#)] [[PubMed](#)]
89. England, R.M.; Rimmer, S. Hyper/highly-branched polymers by radical polymerisations. *Polym. Chem.* **2010**, *1*, 1533–1544. [[CrossRef](#)]
90. Fletcher, N.L.; Houston, Z.H.; Simpson, J.D.; Veedu, R.N.; Thurecht, K.J. Designed multifunctional polymeric nanomedicines: Long-term biodistribution and tumour accumulation of aptamer-targeted nanomaterials. *Chem. Commun.* **2018**. [[CrossRef](#)] [[PubMed](#)]
91. Hörsch, D.; Ezziddin, S. Peptide receptor radionuclide therapy for neuroendocrine tumors in germany: First results of a multi-institutional cancer registry. In *Theranostics, Gallium-68, and Other Radionuclides*; Baum, R., Rösch, F., Eds.; Springer: Berlin, Heidelberg, 2013; pp. 457–465.
92. Zeglis, B.M.; Lewis, J.S. A practical guide to the construction of radiometallated bioconjugates for positron emission tomography. *Dalton Trans.* **2011**, *40*, 6168–6195. [[CrossRef](#)] [[PubMed](#)]
93. Price, E.W.; Orvig, C. Matching chelators to radiometals for radiopharmaceuticals. *Chem. Soc. Rev.* **2014**, *43*, 260–290. [[CrossRef](#)] [[PubMed](#)]

94. Gijs, M.; Dammicco, S. Gallium-68-labelled NOTA-oligonucleotides: An optimized method for their preparation. *J. Label. Compd. Radiopharm.* **2016**, *59*, 63–71. [[CrossRef](#)] [[PubMed](#)]
95. Baes, C.F.; Mesmer, R.S. *The Hydrolysis of Cations*; John Wiley & Sons: Hoboken, NJ, USA, 1976; pp. 318–319.
96. Gijs, M.; Becker, G. Biodistribution of novel <sup>68</sup>Ga-radiolabelled HER<sub>2</sub> aptamers in mice. *J. Nucl. Med. Radiat. Ther.* **2016**, *7*, 300. [[CrossRef](#)]
97. Kang, W.J.; Lee, J. Multimodal imaging probe for targeting cancer cells using umuc-1 aptamer. *Colloids Surf. B Biointerfaces* **2015**, *136*, 134–140. [[CrossRef](#)] [[PubMed](#)]
98. Veedu, R.N. *Aptamers: Tools for Nanotherapy and Molecular Imaging*; CRC Press: Boca raton, FL, USA, 2017; pp. 1–363.
99. Kalia, J.; Raines, R.T. Advances in bioconjugation. *Curr. Org. Chem.* **2010**, *14*, 138–147. [[CrossRef](#)] [[PubMed](#)]
100. Lee, K.Y.; Kang, H. Bioimaging of nucleolin aptamer-containing 5-(n-benzylcarboxamide)-2'-deoxyuridine more capable of specific binding to targets in cancer cells. *J. Biomed. Biotech.* **2010**. [[CrossRef](#)] [[PubMed](#)]
101. Li, W.; Yang, X. Real-time imaging of protein internalization using aptamer conjugates. *Anal. Chem.* **2008**, *80*, 5002–5008. [[CrossRef](#)] [[PubMed](#)]
102. Shi, H.; He, X. Locked nucleic acid/DNA chimeric aptamer probe for tumor diagnosis with improved serum stability and extended imaging window in vivo. *Anal. Chim. Acta* **2014**, *812*, 138–144. [[CrossRef](#)] [[PubMed](#)]



© 2018 by the authors. Licensee MDPI, Basel, Switzerland. This article is an open access article distributed under the terms and conditions of the Creative Commons Attribution (CC BY) license (<http://creativecommons.org/licenses/by/4.0/>).